

AD612797

January 1965

# MEASURING THE ELECTRICAL CHARGE AND VELOCITY OF A MOVING PROJECTILE

By

J. E. NANEVICZ W. C. WADSWORTH

STANFORD RESEARCH INSTITUTE  
MENLO PARK, CALIFORNIA

3158

|            |     |      |   |     |
|------------|-----|------|---|-----|
| COPY       | 2   | OF   | 3 | VLL |
| HARD COPY  | \$. | 2.00 |   |     |
| MICROFICHE | \$. | 0.50 |   |     |

SRI Project 5082

CONTRACT AF 33(615)-1934

## ARCHIVE COPY

MAR 11 1965  
 DEGRA E

Prepared for:

AIR FORCE AVIONICS LABORATORY  
 RESEARCH AND TECHNOLOGY DIVISION  
 UNITED STATES AIR FORCE  
 WRIGHT-PATTERSON AIR FORCE BASE, OHIO

## FOREWORD

---

This report was prepared by Stanford Research Institute, Menlo Park, California, on Air Force Contract AF 33(615)-1934. The work was administered under the direction of the Electromagnetic Environment Branch of the Electronic Warfare Division of the Air Force Avionics Laboratory. Mr. C. R. Austin was the task engineer.

The studies presented began in July 1964 and concluded in January 1965. This represents an effort by the Electronics and Radio Sciences Division of Stanford Research Institute. The principal investigator, Dr. J. E. Nanevich was responsible for research activity under Stanford Research Institute Project 5082.

## ABSTRACT

---

Two different probes were developed for measuring the electrical charge and velocity of a moving charged projectile. The probes were tested using 5/32-inch-diameter steel balls fired from a rifle at roughly 4500 feet per second. The projectiles were frictionally charged to from 50 to 100  $\mu\text{coulomb}$  by passing through a 0.0003-inch-thick plastic sheet.

CONTENTS

---

|                                 |     |
|---------------------------------|-----|
| FOREWORD. . . . .               | ii  |
| ABSTRACT. . . . .               | iii |
| LIST OF ILLUSTRATIONS . . . . . | v   |
| I INTRODUCTION . . . . .        | 1   |
| II INSTRUMENTATION. . . . .     | 3   |
| III EXPERIMENTS. . . . .        | 15  |
| IV CONCLUSIONS. . . . .         | 24  |
| REFERENCES. . . . .             | 25  |

## ILLUSTRATIONS

---

|           |  |    |
|-----------|--|----|
| Fig. 1    | Field of a Charged Particle Moving Between Parallel Planes. . . . .        | 4  |
| Fig. 2    | Possible Probe Design. . . . .   | 6  |
| Fig. 3    | Symmetrical Probe. . . . .   | 7  |
| Fig. 4    | Practical Parallel Plate Probe . . . . .                                   | 8  |
| Fig. 5    | Field Measurement Set-Up . . . . .   | 10 |
| Fig. 6    | Illustrating Arguments Leading to Cylindrical Probe. . . . .               | 12 |
| Fig. 7    | Simple Cylinder Probe. . . . .   | 14 |
| Fig. 8    | Improved Cylinder Probe. . . . .   | 14 |
| Fig. 9(a) | Photograph of Laboratory Set-Up Viewed from Rifle End. . . . .             | 16 |
| Fig. 9(b) | Photograph of Laboratory Set-Up Viewed from Electrode End. . . . .         | 17 |
| Fig. 10   | Set-Up for Testing Projectile Discharging and Charging Techniques. . . . . | 18 |
| Fig. 11   | Set-Up for Demonstrating Successive Charging of Projectile. . . . .        | 19 |
| Fig. 12   | Set-Up for Probe Comparison. . . . .                                       | 21 |
| Fig. 13   | Set-Up for Tracking Projectile . . . . .                                   | 22 |

## I INTRODUCTION

In studying the problem of vehicle-induced electromagnetic interference on a low-altitude, long-range, all-weather vehicle operating in the speed range Mach 3 to Mach 10, it is necessary to investigate the manner in which frictional "triboelectric" charging of the vehicle by precipitation particles varies with speed.<sup>1,2,3\*</sup> Although the charging rate may be deduced from the particle density, the charge acquired by each particle, and the effective intercept area of the vehicle, it is important that precipitation charging rates be determined experimentally because of particle shattering, frontal heating, and uncertainties regarding the applicability of theoretical data on spherical water droplet impingement<sup>4,5,6</sup> to ice crystals. Since no available vehicles operate in this speed range at the altitudes of interest, flight test measurements of charging rate in this speed regime were not possible.

It was decided that the experiments would be made in a refrigerated chamber, in which an ice fog would be produced by injecting steam and seeding with dry ice. From a study of the charge acquired by a projectile traveling through this ice fog, the charging rate could be deduced. In addition, with the proper experimental technique, it should be possible to obtain useful data on the effective intercept area of the projectile and on individual particle charge.

To move it through the ice fog, the projectile could be mounted on the end of a rotating, aerodynamically shaped radius arm in a manner similar to that used by Stimmel,<sup>7</sup> or the projectile could be fired through the chamber in the manner of a rifle bullet. The latter approach appears to be the most promising, since most of the speed range of interest can easily be achieved with relatively inexpensive apparatus. The charge acquired by the projectile will be determined by measuring

---

\*References are listed at the end of the report.

the interaction of the charge with electrode structures located along the path of the projectile. By using several such detectors, the change in projectile charge can be determined for a known distance traveled between electrodes. In addition, by measuring the time between the interaction with succeeding electrodes, the velocity of the projectiles can be accurately determined. A reference projectile will be fired at a fixed velocity, so that variations in the properties of the ice fog from one test to the next will not be misinterpreted. Particle density will be determined by photographing the particles illuminated by a collimated beam of light and counting the particles in a given length of the beam.

This report describes the development and testing of the electrodes and associated instrumentation required to perform measurements on moving charged projectiles. Although the present application of these techniques is a very specialized one, the techniques themselves are of general interest.

## II INSTRUMENTATION

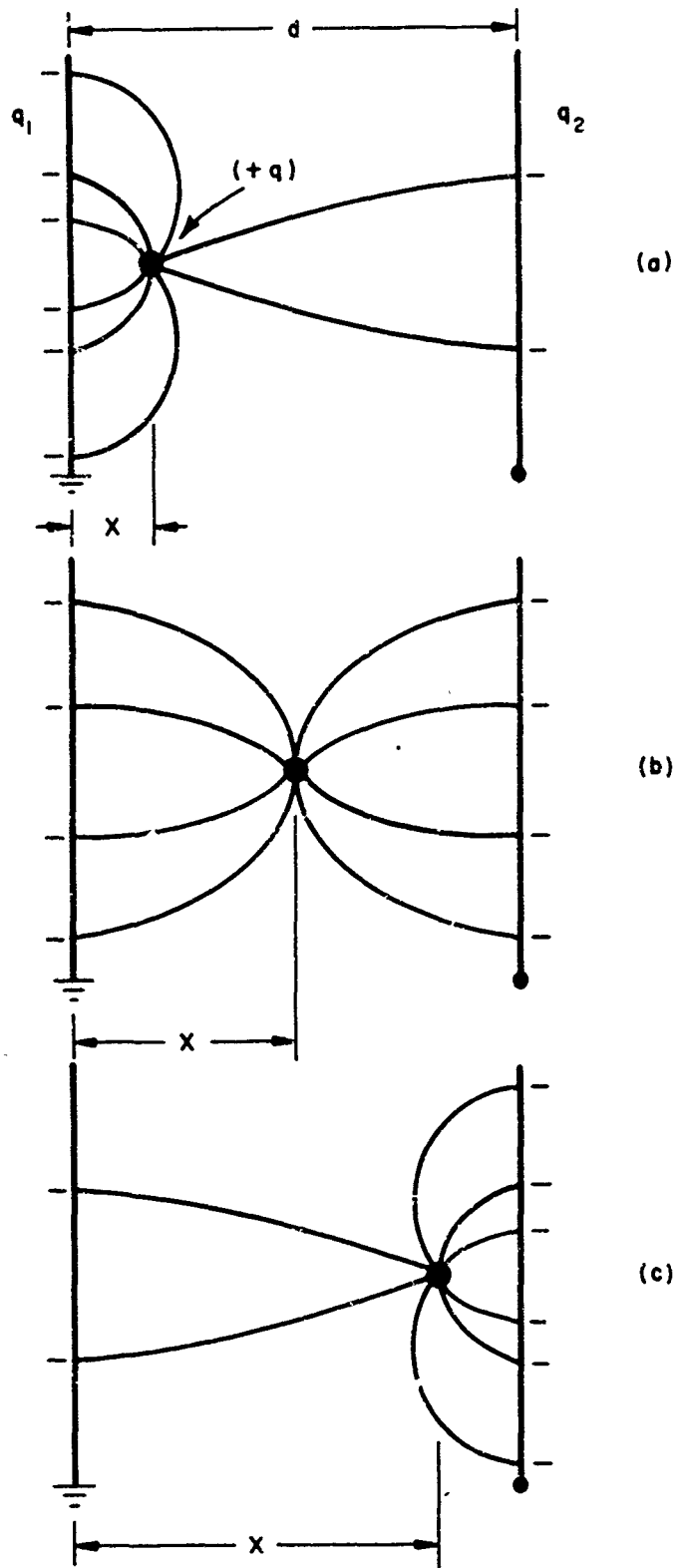
It has been shown<sup>1,8,9,10,11</sup> that if a charged particle moves in the vicinity of a set of electrodes, the instantaneous terminal current induced in one of the electrodes is given by

$$i = \frac{qv E_v}{V} \quad (1)$$

where  $q$  is the charge on the particle,  $v$  is its instantaneous velocity, and the reciprocal field  $E_v$  is the component in the direction  $v$  of that electric field which would exist at the instantaneous position of the particle under the following circumstances: the charged particle is removed; the given electrode is raised to potential  $V$ ; and all other conductors are grounded. In the case of a charged particle moving between a pair of parallel plates, the reciprocal field  $E_v$  is given simply by  $E_v = V/d$  so that Eq. (1) reduces to

$$i = \frac{qv}{d} \quad (2)$$

The validity of this result is readily verified by the following simple argument, which is included here for the sake of completeness: shown in Fig. 1 is the sequence of events as a charged particle moves from one to the other of a set of parallel plates. Emanating from the particle are  $q$  lines of flux which terminate on an equal amount of negative charge on the two electrodes. When the particle is near the left plate, as in Fig. 1(a), most of the lines terminate on the left plate so that very little charge is induced on the right electrode. When the particle is midway between the two plates, as in Fig. 1(b), one half of the particle charge is induced on the right electrode.



TA-5082-1

FIG. 1 FIELD OF A CHARGED PARTICLE MOVING BETWEEN PARALLEL PLANES

When the particle is nearer the right plate as in Fig. 1(c), the induced charge on the right electrode approaches the particle charge.

The numerical magnitude of the induced charge described above may be determined by assuming that the right plate is at a potential  $V$ , and equating the work done in transferring charge from the left to the right plate to the energy lost by the particle in its movement. The work done in transferring a charge  $q_2$  from the left to the right plate through a potential difference  $V$  is given by  $Vq_2$ . At the same time, the particle has moved a distance  $x$  against a field of magnitude  $V/d$  and has therefore lost an amount of energy given by  $q \times V/d$ . Therefore,

$$Vq_2 = \frac{q \times V}{d}$$

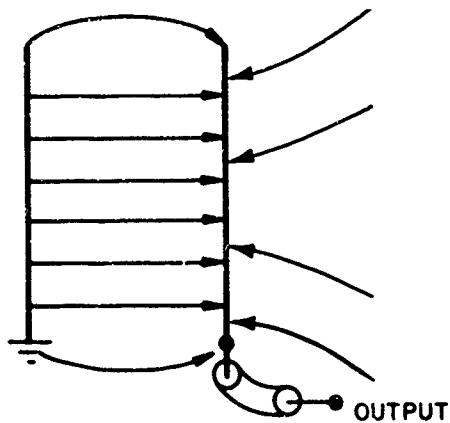
$$q_2 = \frac{q \times x}{d}$$

But the current associated with the induced charge resulting from the moving particle is given simply by the time rate of charge. Thus

$$i = \frac{dq_2}{dt} = \frac{q}{d} \frac{dx}{dt} = \frac{qv}{d}$$

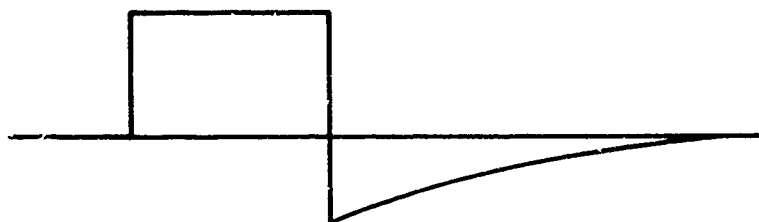
which is in agreement with Eq. (2).

The above results suggest that a probe suitable for studying moving charged projectiles might be designed as shown in Fig. 2(a). Since the reciprocal field  $E_v$  between the plates is uniform, a positively charged projectile moving from left to right with constant velocity in this region will produce a steady positive output current as shown in the left-hand portion of Fig. 2(b). To the right of the output electrode, the direction of the reciprocal field is reversed, its magnitude is



(a)

RECIPROCAL FIELD STRUCTURE ABOUT ELECTRODES



(b)

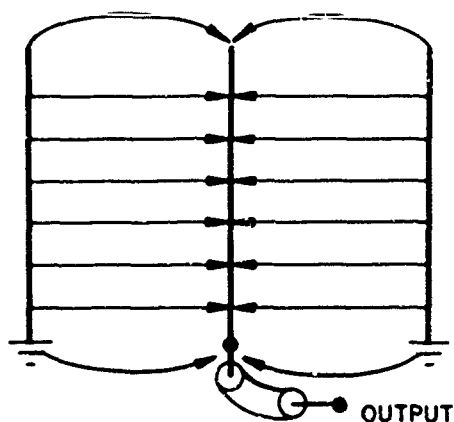
OUTPUT CURRENT

TA-5082-2

FIG. 2 POSSIBLE PROBE DESIGN

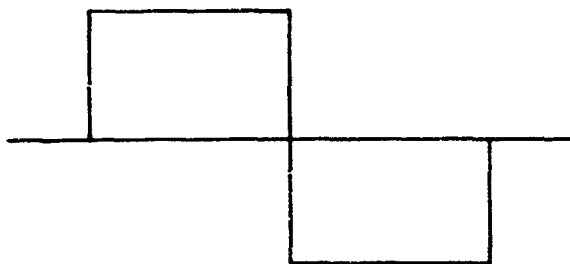
reduced, and the magnitude of the field varies with distance from the output plate. Thus, upon emerging from the output electrode, the projectile produces a varying negative output current which persists until the projectile is far from the electrode.

A somewhat improved probe design (in that the fields on both sides of the output electrode are well defined) is shown in Fig. 3(a). The output signal produced by a positively charged projectile moving at constant velocity from left to right is shown in Fig. 3(b). Its form can be deduced from the following arguments: Prior to passing the first grounded plate, the projectile is shielded from the output electrode and induces no signal in it. Upon passing the first electrode, the projectile is in a uniform reciprocal field and produces a constant positive output signal. After passing the output electrode, the projectile is in a uniform reciprocal field of opposite sign and produces



(a)

RECIPROCAL FIELD STRUCTURE ABOUT ELECTRODES



(b)

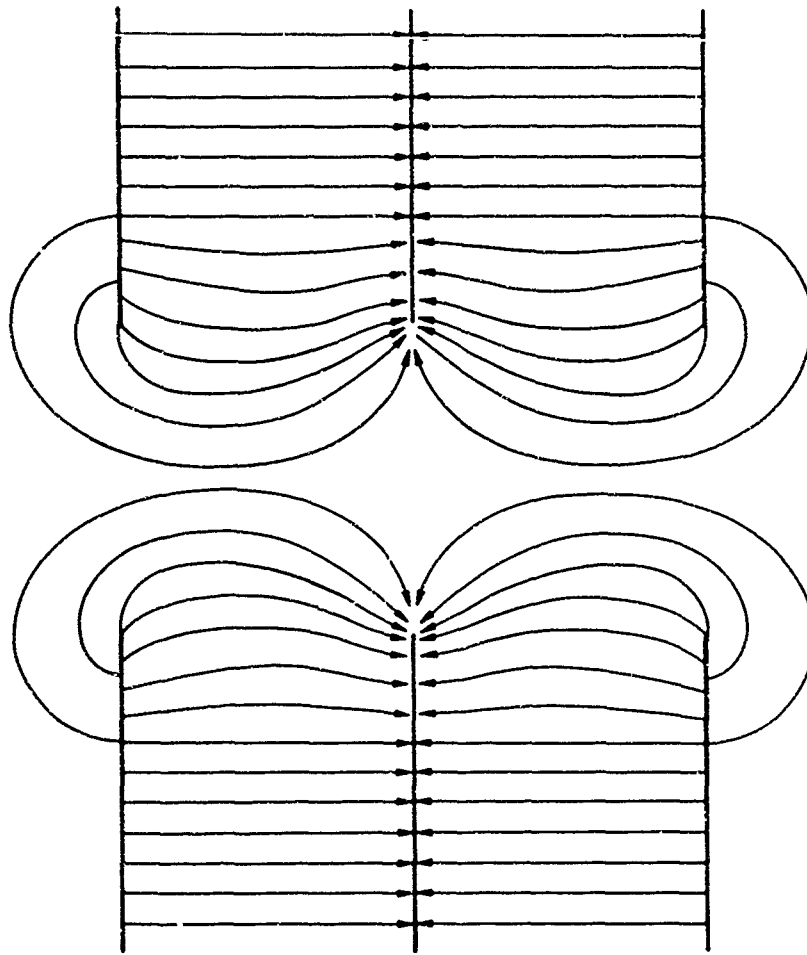
OUTPUT CURRENT

TA-5082-3

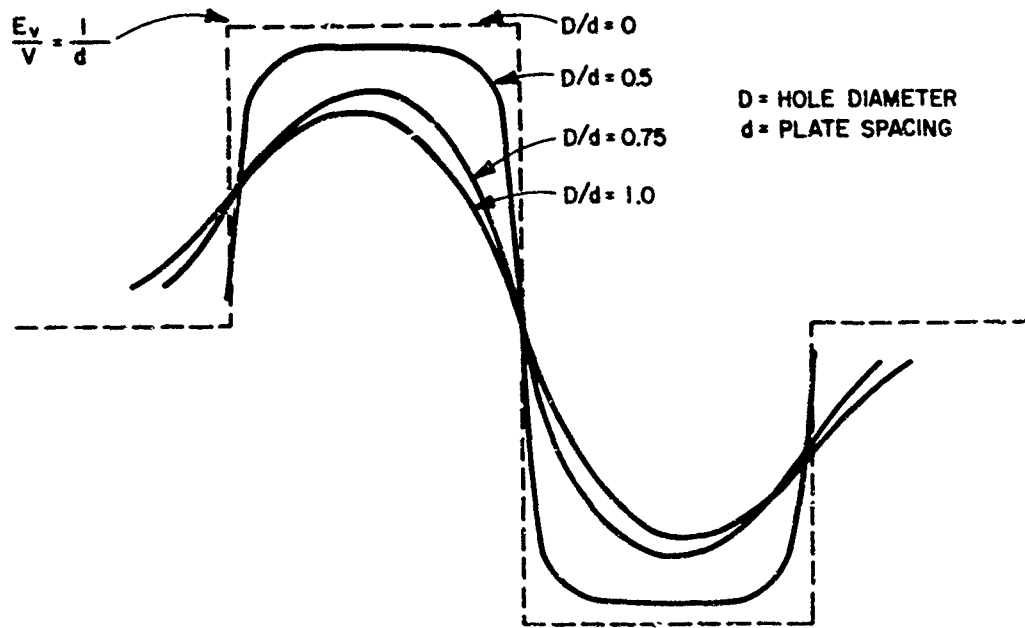
FIG. 3 SYMMETRICAL PROBE

a negative output signal. Upon passing the second grounded plate, the projectile is again shielded from the output electrode and induces no signal in it.

The probes shown in Figs. 2 and 3 are idealized and cannot be used in practice since they do not incorporate openings through which the projectile can pass. A practical probe design, together with a rough sketch of its reciprocal field structure, is shown in Fig. 4(a). The probe illustrated is one in which the diameter of the hole through the electrodes equals the electrode spacing. (This probe geometry was used in the experiments described in Sec. III.) It is evident from the field structure that  $E_v$  along the centerline of the hole is everywhere lower than the undisturbed field between the plates. Furthermore,  $E_v$  along the centerline varies with position, and as the result of field fringing,



(a) FIELD STRUCTURE



(b) OUTPUT CURRENT

TR-5082-4

FIG. 4 PRACTICAL PARALLEL PLATE PROBE

is not zero outside the plates. The output current waveform which would be obtained from a probe of this design is illustrated in Fig. 4(b) for various ratios of hole diameter to plate spacing. Also shown in the figure is the output signal from an idealized probe having an infinitesimal hole for the passage of the projectile. Comparison of the pulses indicates, for example that for a practical probe with  $D/d = 1$  (a hole diameter to spacing ratio of unity) the peak current is 0.72 of the peak current from the idealized parallel plate probe. The pulse form is obviously quite different from that obtained from an idealized probe.

Data for the output current pulse of Fig. 4(b) were obtained using a 12:1 scale model of the probe structure by moving a spark discharge signal from point to point between the probe electrodes and reading the amplitude of the current pulse induced in the electrodes. The laboratory set-up used in making these measurements is shown in Fig. 5. The resistance of the leads to the spark gap is sufficiently high that the leads are transparent to the RF reciprocal fields existing between the plates. Thus, the signal source appears as a spark occurring between a pair of completely isolated balls, which can be moved from place to place. Its presence produces virtually no distortion in the field being measured.

It has been shown<sup>2,12,13</sup> that the signal induced in the electrode structure by the spark discharge is given by

$$i = \frac{E_v}{V} \int f(z) J(z) dz \quad (3)$$

where  $i$ ,  $E_v$ , and  $V$  are as defined for Eq. (1),  $J(z)$  describes the current in the spark gap, and  $f(z)$  is the function relating the field within the spark gap to the field  $E_v$  which we wish to measure as follows:

$E_{\text{gap}}(z) = f(z) E_v(z)$ . Essentially, the integral describes the signal generated by the spark source. Since the same spark source is used for

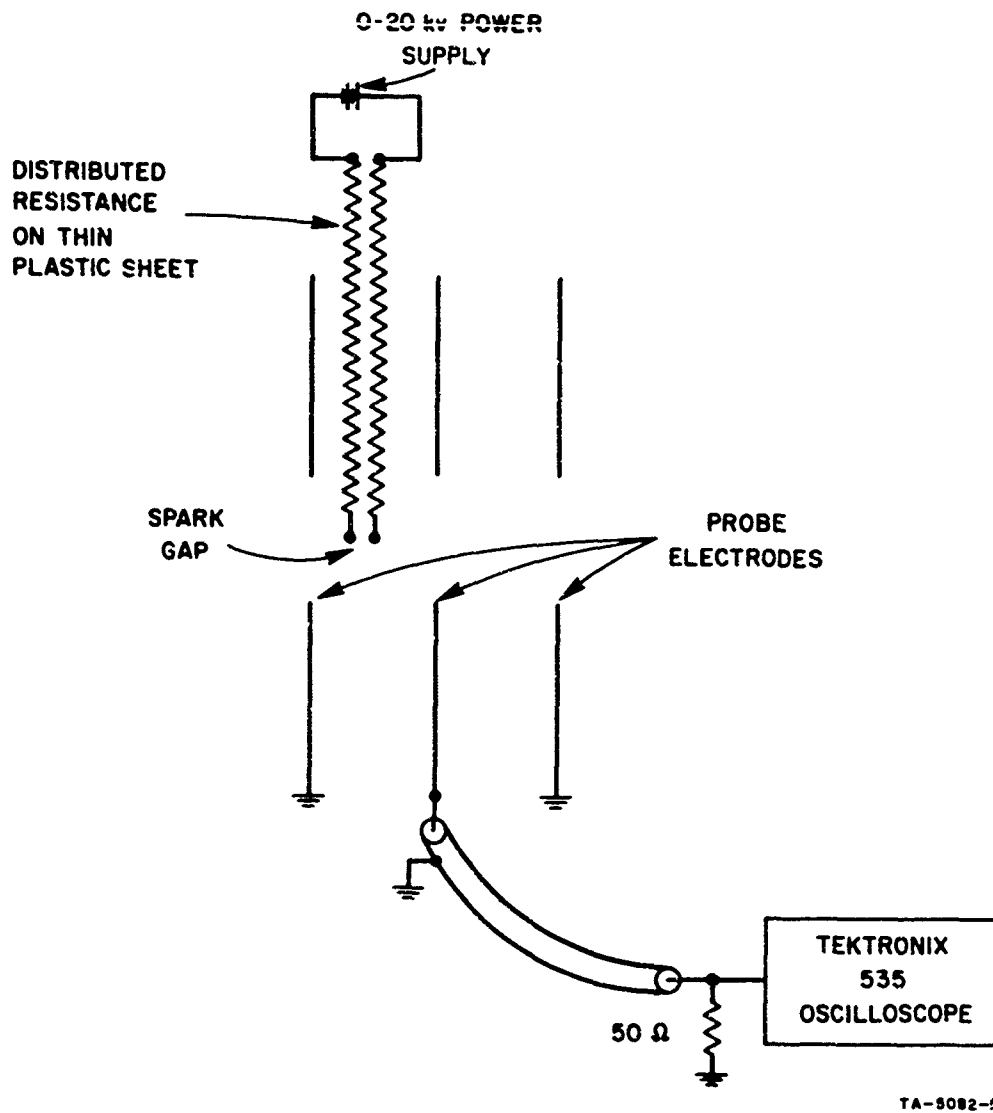


FIG. 5 FIELD MEASUREMENT SET-UP

the measurements at all points, the integral does not vary; therefore, variations occurring in  $i$  as the spark source is moved from point to point indicate changes in reciprocal field  $E_v$ .

In conducting the field studies, a preliminary measurement was made in which aluminum foil sheets were placed over the holes in the electrodes to produce the idealized structure in which  $E_{v1} = V/d$ . When the spark discharge was placed between the plates, pulses of amplitude  $h_1$  were observed on the oscilloscope. Next, the aluminum foil sheets were removed and measurements were made with the spark held at positions of interest in the practical electrode configuration. In this case the

spark discharge produced pulses of amplitude  $h_2(z)$  on the oscilloscope. The normalized reciprocal field  $E_{v2}(z)/V$  at a particular point  $z$  along the centerline of the practical probe is found from

$$\frac{h_2(z)}{h_1} = \frac{E_{v2}(z)}{E_{v1}}$$

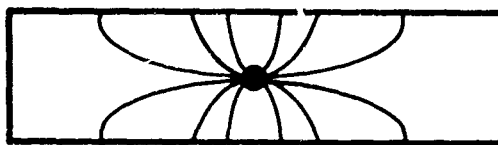
or

$$\frac{E_{v2}(z)}{V} = \frac{1}{d} \frac{h_2(z)}{h_1} \quad (4)$$

The probe illustrated in Figs. 4 and 5 is simple to fabricate and use, and has the desirable feature that the polarity of the output current changes sign during the pulse. This zero crossing is very clearly defined in oscillograms, and facilitates the accurate determination of projectile velocity by measuring the time between zero crossings of pulses produced from two probes spaced a known distance along the projectile trajectory.

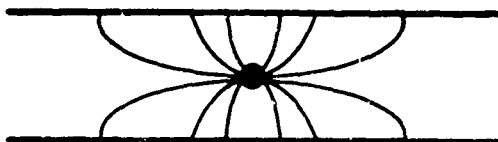
Inherent in the derivation of Eqs. (1) and (2) is the assumption that the charged body is of infinitesimal dimensions so that its introduction into the region between the electrodes of the probe will not appreciably affect the field configuration. Thus the probe calibration of Fig. 4(b) is valid only for projectiles that are much smaller than the spacing between the electrodes. Unfortunately, as the program progressed, it was found that the requirement for projectile stability would make it necessary to use projectiles roughly 3/4 inch long. The presence of so large a body would certainly modify the reciprocal field structure of the probe, with its electrode spacing of one inch. Furthermore, both the peak current and its waveform would be modified by changes in projectile dimensions so that it would be necessary to determine a new calibration for each projectile design.

A second "cylindrical" probe type was also investigated. The arguments leading to its design are illustrated in Fig. 6. If a particle



(a)

CHARGED PARTICLE INSIDE CLOSED CYLINDRICAL BOX



(b)

CHARGED PARTICLE INSIDE OPEN ENDED CYLINDER

TA-5082-6

FIG. 6 ILLUSTRATING ARGUMENTS LEADING TO CYLINDRICAL PROBE

bearing a positive charge  $q$  is placed within a capped cylindrical tube as in Fig. 6(a), the field lines emanating from the particle terminate on an equal amount of negative charge on the inner wall of the tube. Thus the box is left with a net positive charge  $q$  on its outer surface. If the tube is sufficiently long as is illustrated in Fig. 6(a), very few lines terminate on the end caps. In this case, the end caps can be removed (to permit the passage of a projectile) without appreciably altering the total charge on the cylinder.

The charge on the particle may be determined simply by measuring the potential of the cylinder when the particle is inside, since

$$q = CV \quad (5)$$

where  $q$  is the charge on the surface of the cylinder,  $V$  is the potential of the cylinder, and  $C$  is the capacitance to ground of the cylinder and the wiring used to connect it to the measuring system. In designing the associated instrumentation, it is essential to be certain that the resistance  $R$  to ground of the cylinder is sufficiently high that  $RC$  is much greater than the time required to perform a measurement. Otherwise sufficient current will flow to the cylinder to neutralize an appreciable fraction of the charge on its surface, thereby invalidating the charge measurement. Since we are interested here in measuring the charge on a moving projectile, it is necessary that  $RC$  be much greater than the time that the projectile spends inside the cylinder, or

$$RC \gg l/v \quad (6)$$

where  $l$  is the cylinder length, and  $v$  is projectile velocity.

Since the charge induced on the outer surface of the cylinder does not depend upon the details of field structure between the projectile and the inner cylinder walls (provided only that the cylinder is sufficiently long), the peak voltage out of the system is independent of projectile form. This overcomes the main objection to the parallel plate probe.

A drawback of the cylindrical probe is that its output signal does not change polarity during the passage of the projectile, so that there is no clearly defined point on the pulse from which to make time measurements for velocity determination. In addition, if a simple cylinder is used as a probe, as shown in Fig. 7, some charge will be induced on the cylinder and an output signal will be obtained long before the projectile enters the cylinder. A rounded pulse of this sort is particularly undesirable for velocity measurements. Considerable improvement in the pulse shape can be achieved by the addition of a grounded plate on either side of the cylinder, as shown in Fig. 8. This results in a much more

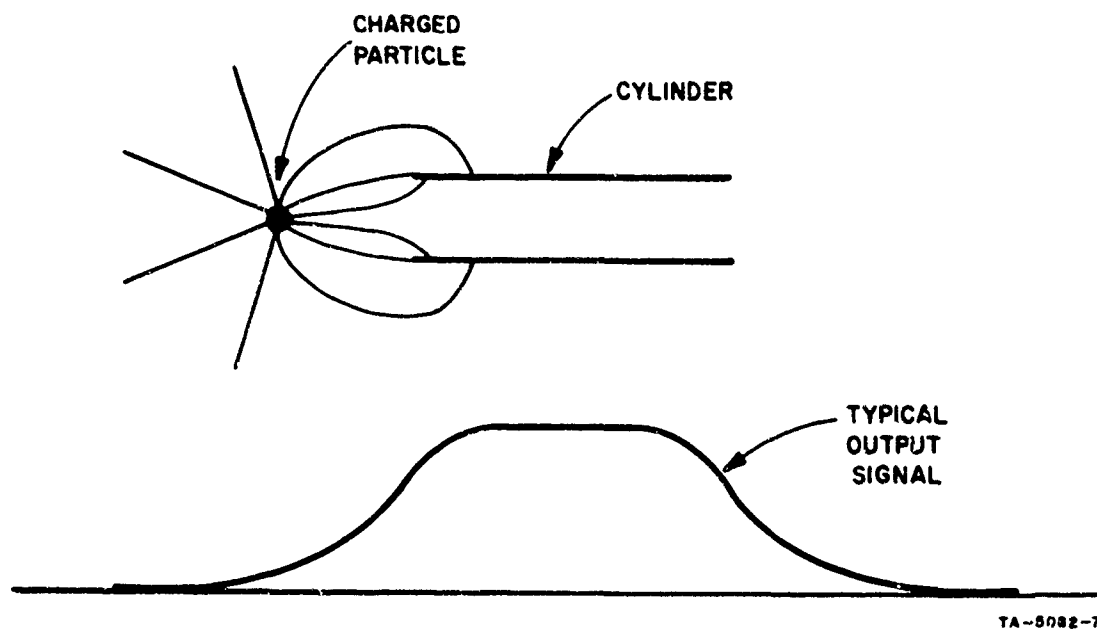


FIG. 7 SIMPLE CYLINDER PROBE

accurately defined field geometry for the probe. With the conducting plates in place, virtually no charge is induced on the cylinder until the projectile passes through the first plate, and the rise and decay times of the pulse are greatly reduced as a result. A rapid rise and decay are desirable for accurate timing.

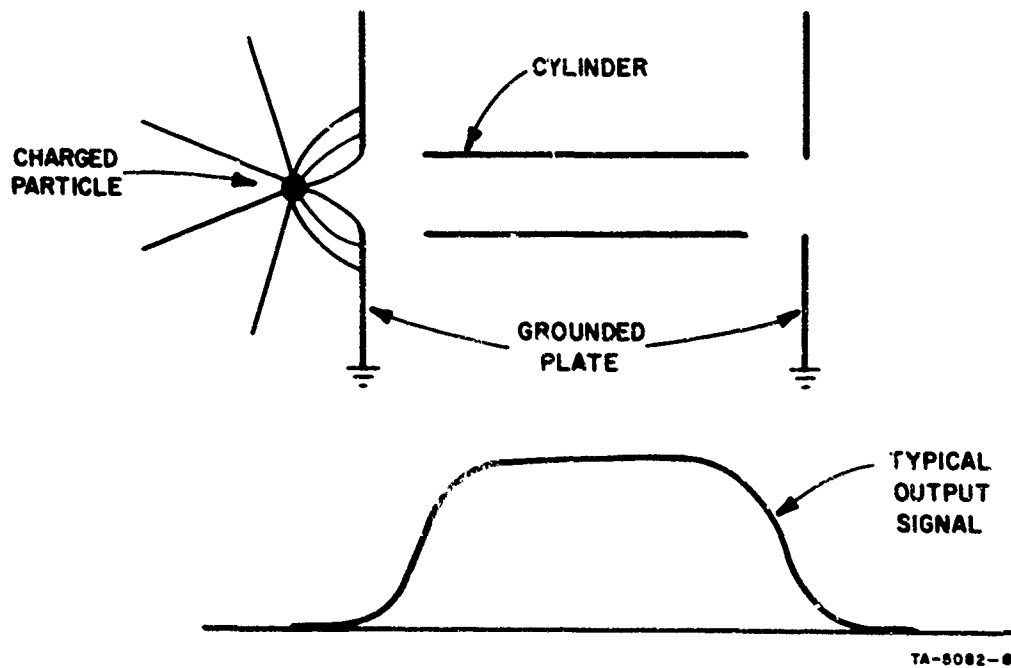


FIG. 8 IMPROVED CYLINDER PROBE

### III EXPERIMENTS

The experiments conducted thus far have been intended to test the probes and associated instrumentation that will be used in the refrigerated chamber to study the charging of fast-moving objects. A typical laboratory set-up is shown in Fig. 9. For the test illustrated, the projectile was a 5/32-inch-diameter steel ball held in an aluminum sabot while in the rifle barrel. After leaving the barrel, the sabot split in two and was stopped by the 1/2-inch thick steel sabot stripper. The projectile passed through the plates of the gas stripper where it lost most of the accompanying slug of gas. Upon leaving the gas stripper the projectile broke an aluminum ribbon triggering the oscilloscopes. Next, the projectile passed through a ring stand which was used to support various metal and plastic materials to discharge or charge the projectile. Finally, the projectile passed through the instrumentation probes.

In the experiment shown in Fig. 10, an investigation was made of the effectiveness of an aluminum foil sheet in discharging the projectile before it entered the test region. Upon breaking the trigger ribbon, the projectile penetrated the grounded aluminum foil intended to remove any charge existing on the projectile. The magnitude of the signal induced in the first probe assembly (shown in the top trace of the oscillogram) is proportional to the charge on the projectile upon leaving the aluminum foil sheet. The foil is evidently very effective in discharging the projectile since no signal was obtained.

Upon leaving the first probe the projectile penetrated a polyethylene sheet intended to simulate the frictional charging resulting from impact with ice crystals. The charge thus acquired by the projectile induced the signal shown in the bottom trace during passage through the second probe. This experiment demonstrated that it is possible to adequately discharge the projectile after it leaves the rifle barrel, and that easily measurable signals are generated in the test instrumentation following frictional charging of the projectile.

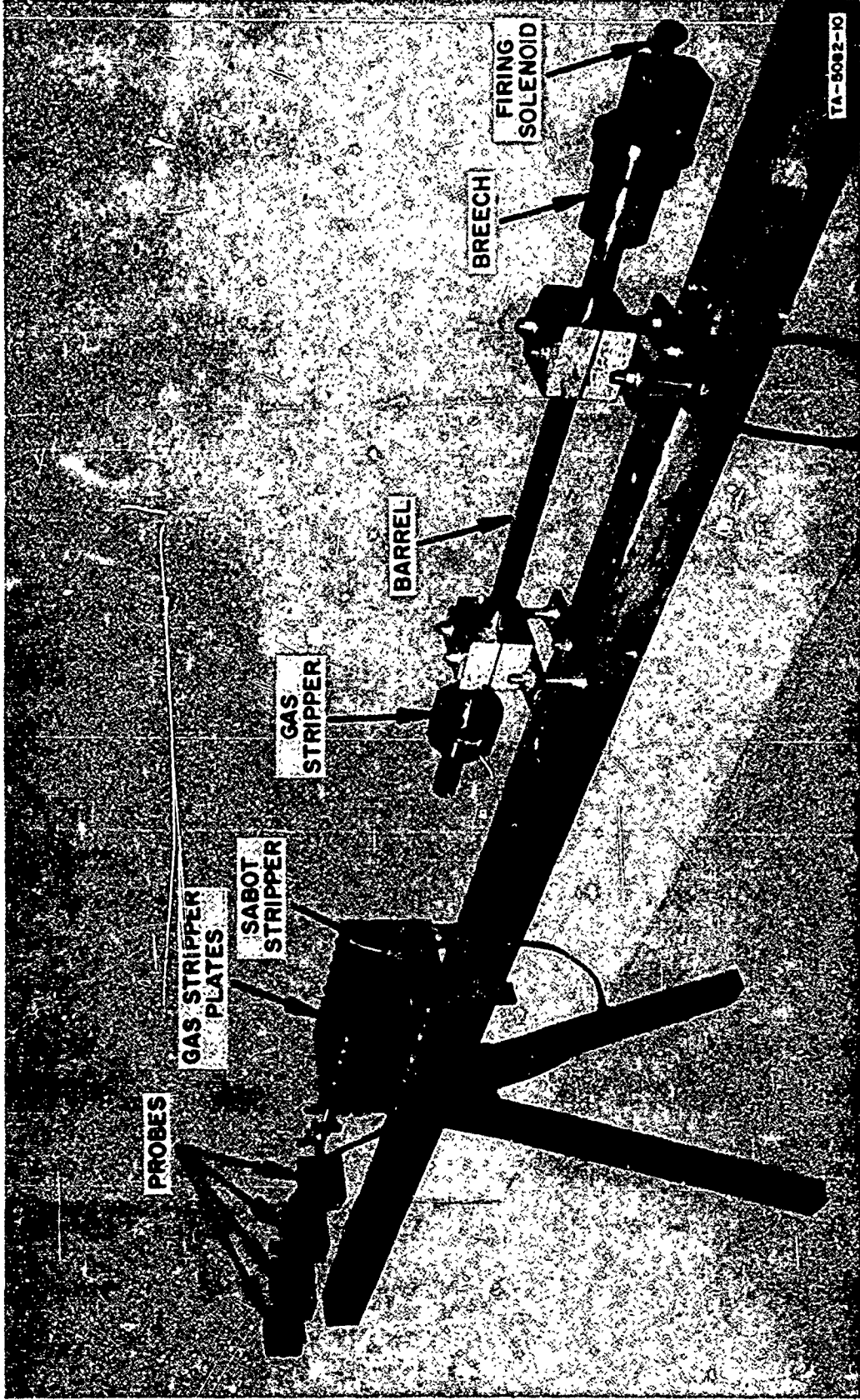


FIG. 9(a) PHOTOGRAPH OF LABORATORY SET-UP  
(Viewed from Rifle End)

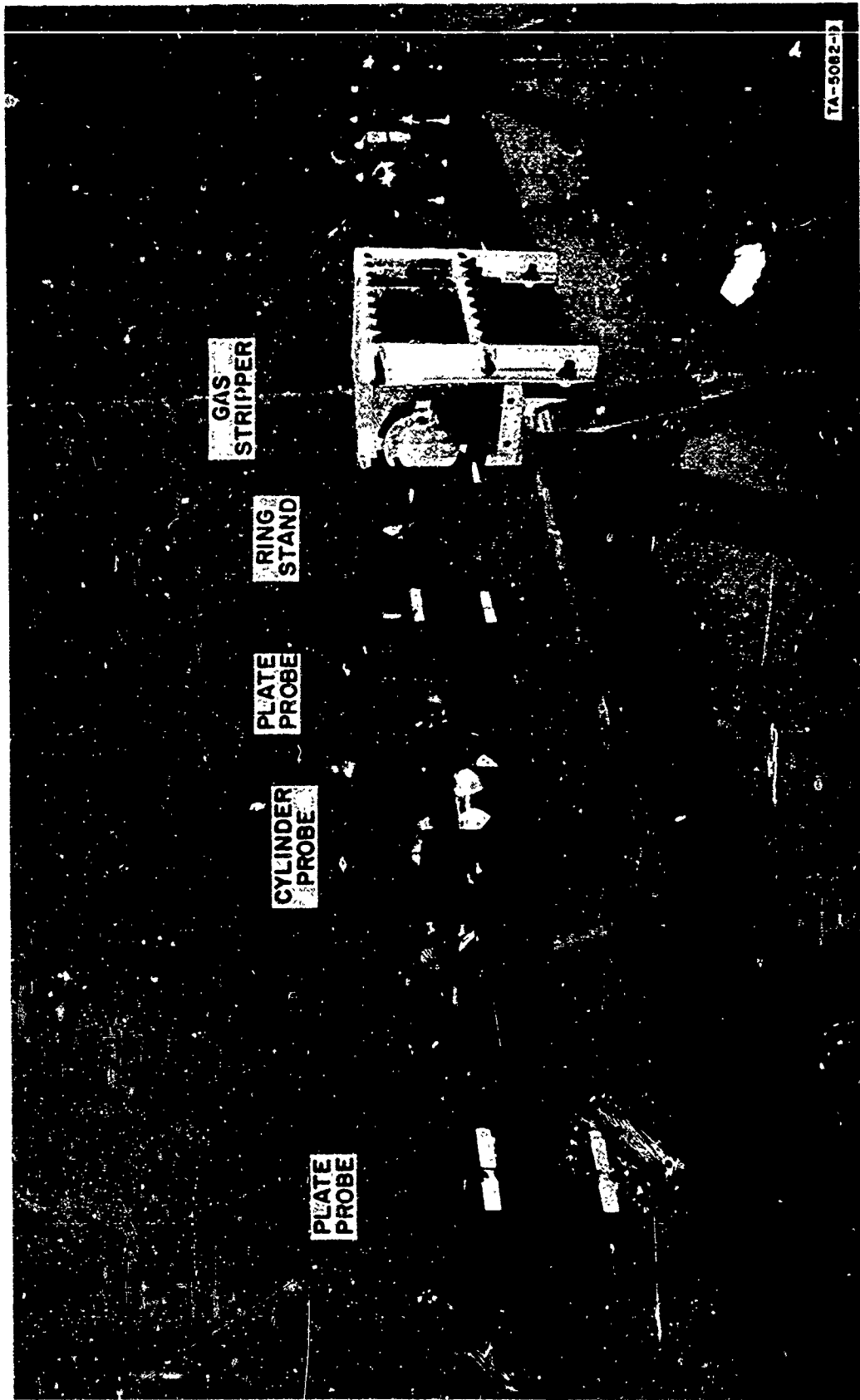


FIG. 9(b) PHOTOGRAPH OF LABORATORY SET-UP  
(Viewed from Electrode End)

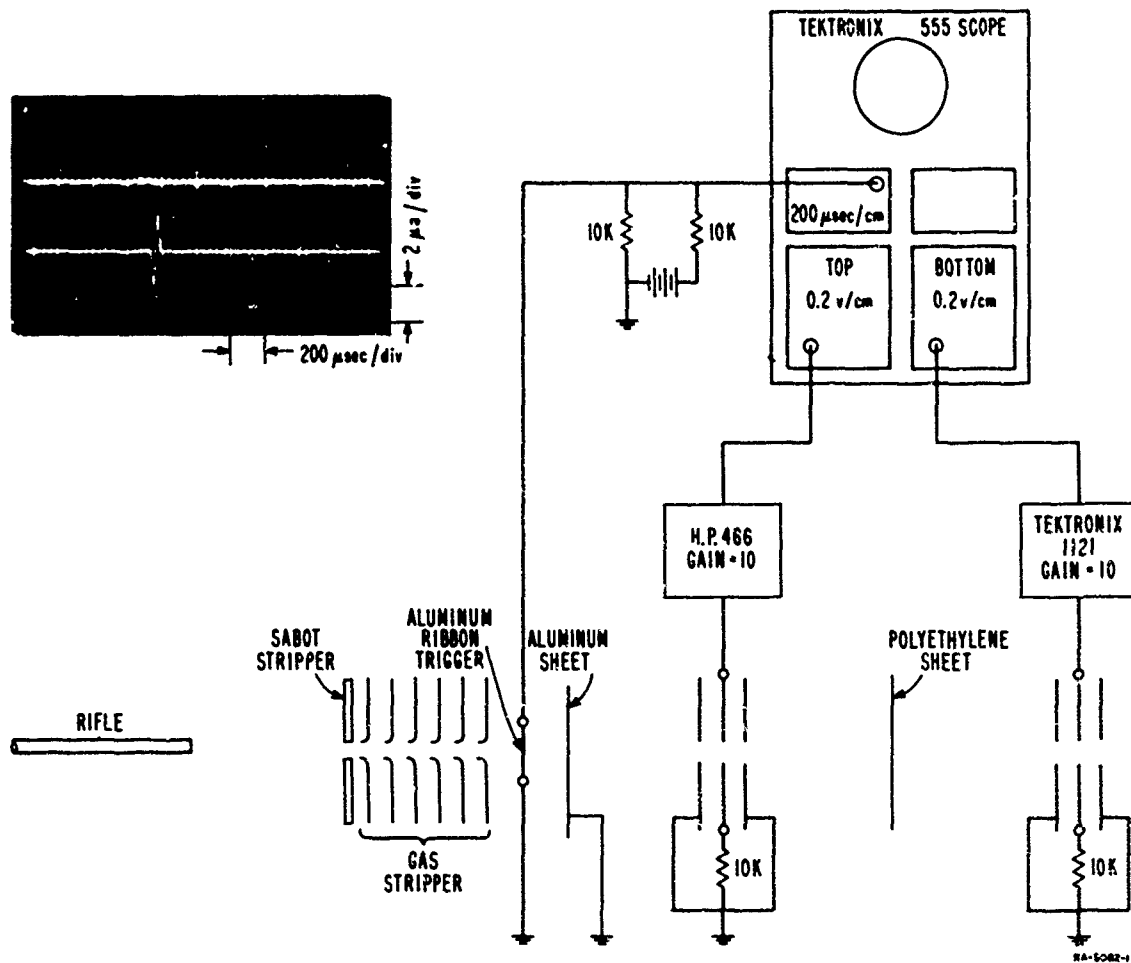


FIG. 10 SET-UP FOR TESTING PROJECTILE DISCHARGING AND CHARGING TECHNIQUES

In another experiment, illustrated in Fig. 11, it was possible to measure projectile velocity and to measure the additional charge acquired by a previously charged projectile. In this set-up, the projectile was charged by a Mylar sheet prior to entering the first probe, producing the top trace in the oscillogram. It acquired additional charge upon striking a second Mylar sheet prior to entering the second probe (lower trace on oscillogram). Since the two probes were 2 feet apart, and since the two pulses are spaced in time by roughly 400 μsec, the projectile velocity was 5000 ft/sec or  $1.525 \times 10^5$  cm/sec.

From the top trace on the oscillogram we find that the projectile induced a peak short-circuit current of  $i_{\max} = 3.3 \times 10^{-6}$  amp in the first probe. In the probe used for these experiments the plate spacing  $d$  was 1 inch and the hole diameter  $D$  was 1/2 inch. From Fig. 4 for

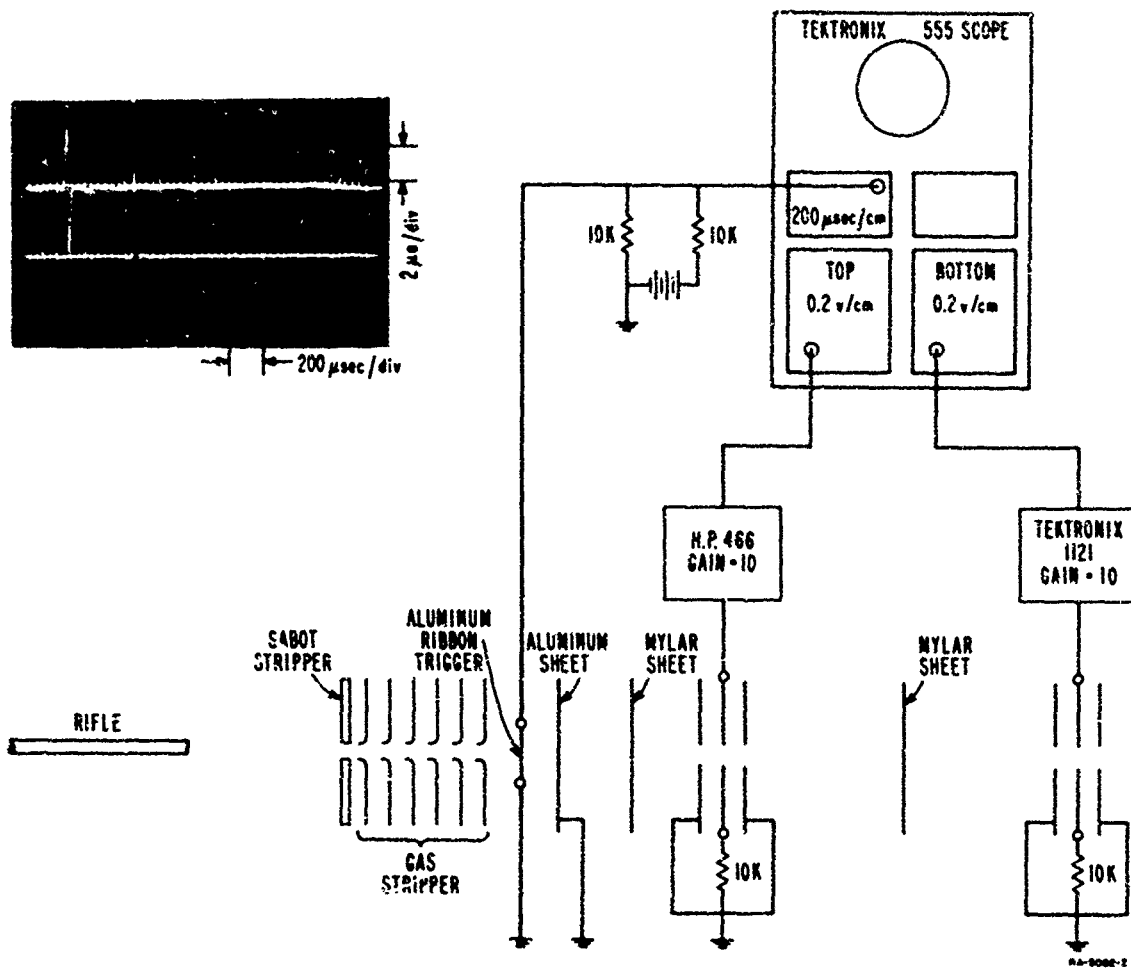


FIG. 11 SET-UP FOR DEMONSTRATING SUCCESSIVE CHARGING OF PROJECTILE

$D/d = 0.5$ , we find that  $\frac{E}{v \max} = 0.933/d$ . Rewriting Eq. (1) we obtain

$$q = \frac{i V}{v E} \quad (7)$$

which, upon substituting numerical values, yields for the charge on the projectile upon entering the first probe,

$$q = \frac{3.3 \times 10^{-6} (2.54)}{1.525 \times 10^5 (0.933)}$$

$$= 59 \mu\text{coulomb (positive)}$$

Similarly the charge upon entering the second electrode was  $86.3 \mu\text{coulomb}$ .

Substituting the charge value of  $q = 59 \mu\text{coulomb}$  and a projectile radius of  $r = 5/64$  inch into

$$E = \frac{q}{4\pi \epsilon r^2} \quad (8)$$

we find that the field intensity at the surface of the ball is  $E = 1.36 \times 10^5$  volts/meter. This is considerably below the corona threshold field of  $3 \times 10^6$  volts/meter. Thus with this charge magnitude there should be no problem with loss of charge from the projectile as the result of corona discharge.

It is of interest to compare the projectile charge magnitude obtained in the simulation experiments where the projectile is fired through a plastic sheet with the charge magnitudes expected in the refrigerated chamber. From Ref. 1 we find that, for the ice fog crystals generated in a refrigerated chamber, the charge per crystal impact is roughly  $10^{-13}$  coulomb and that the crystal concentration is roughly  $10^8$  crystals/ $\text{m}^3$ . In moving 0.5 meter through the chamber, a 5/32-inch-diameter ball will sweep out a volume of  $6.15 \times 10^{-6}$  meter<sup>3</sup> and will therefore acquire a charge of  $6.15 \times 10^{-11}$  coulomb, which is of the same order of magnitude as the charge obtained in the present experiments. Thus the instrumentation should certainly have adequate sensitivity to permit measurements in the refrigerated chamber.

The potential of this ball at the position of the first probe may be found by substituting the projectile radius and charge value  $q = 59 \mu\text{coulomb}$  into

$$\begin{aligned} V &= \frac{q}{4\pi \epsilon r} \\ &= 268 \text{ volts} \end{aligned} \quad (9)$$

The experiment illustrated in Fig. 12 was intended to compare the results obtained with the two probe types. From the pulse spacings we find that the projectile velocity was 4910 feet/sec or  $1.373 \times 10^5$  cm/sec. The projectile charge may be found from the peak signal induced in the parallel plate probes (top trace in the oscillogram) using Eq. (7) as before except that for this experiment the probe hole diameter was  $D = 1$  inch while the plate spacing  $d = 1$  inch so that the data for  $D/d = 1$  in Fig. 4 must be used in determining  $\frac{E_v \max}{v} = \frac{0.73}{d}$ . The projectile charge determined from the parallel plate probe is  $q = 89.1$   $\mu$ coulomb.

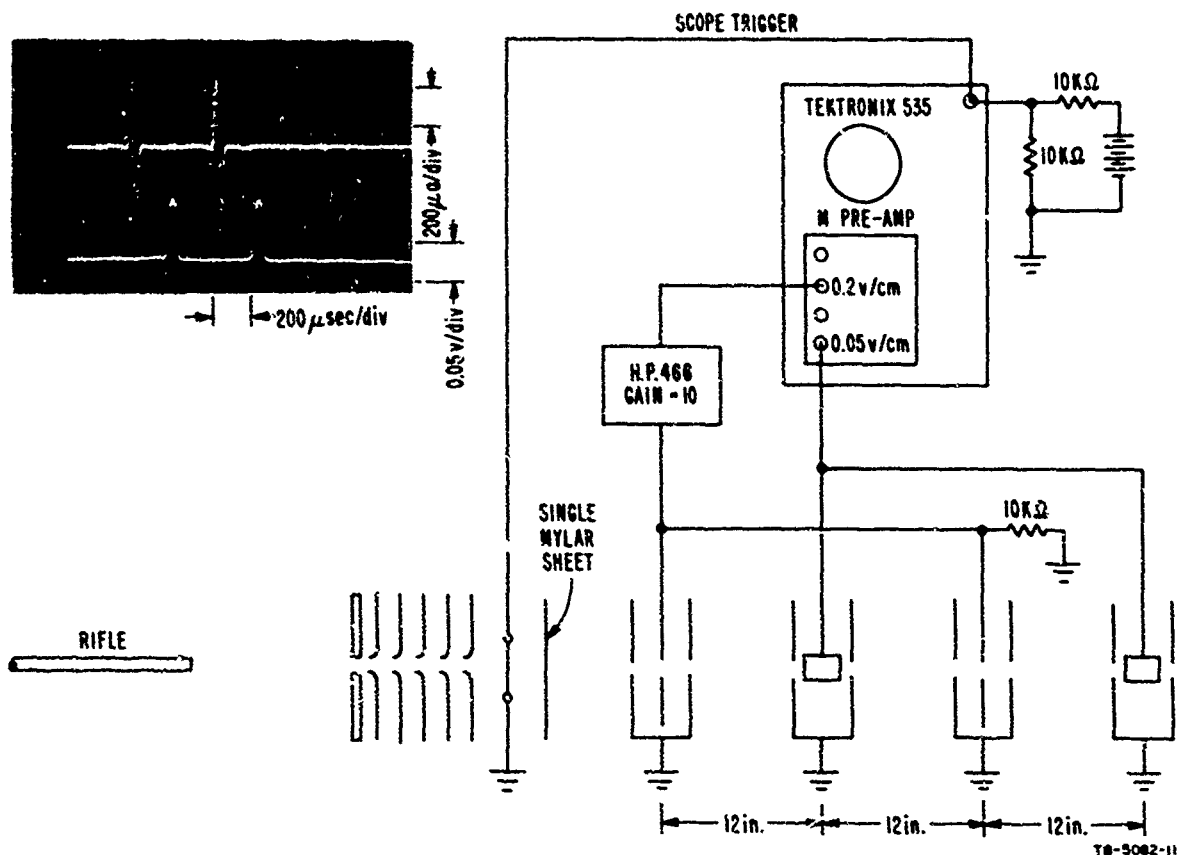


FIG. 12 SET-UP FOR PROBE COMPARISON

From the lower trace in the oscillogram we find that the peak voltage induced in the cylindrical probe is 0.075 volt. Capacitance measurements on the experimental set-up indicated that the total probe capacitance to ground (including cables and instrumentation) was

$C = 1188 \mu\text{fd}$ . Substituting these numbers into Eq. (5) we find that

$$q = 0.075 (1.188 \times 10^{-9})$$

$$= 89.3 \mu\mu\text{coulomb}$$

which is in good agreement with the charge magnitude derived from the parallel plate probe. (It is worth noting that since the peak signal produced in the cylindrical probe is independent of projectile velocity, projectile charge may be determined by using only a single probe.)

In the experiment illustrated in Fig. 13, a series of four cylindrical probes were arranged along the projectile path to present a

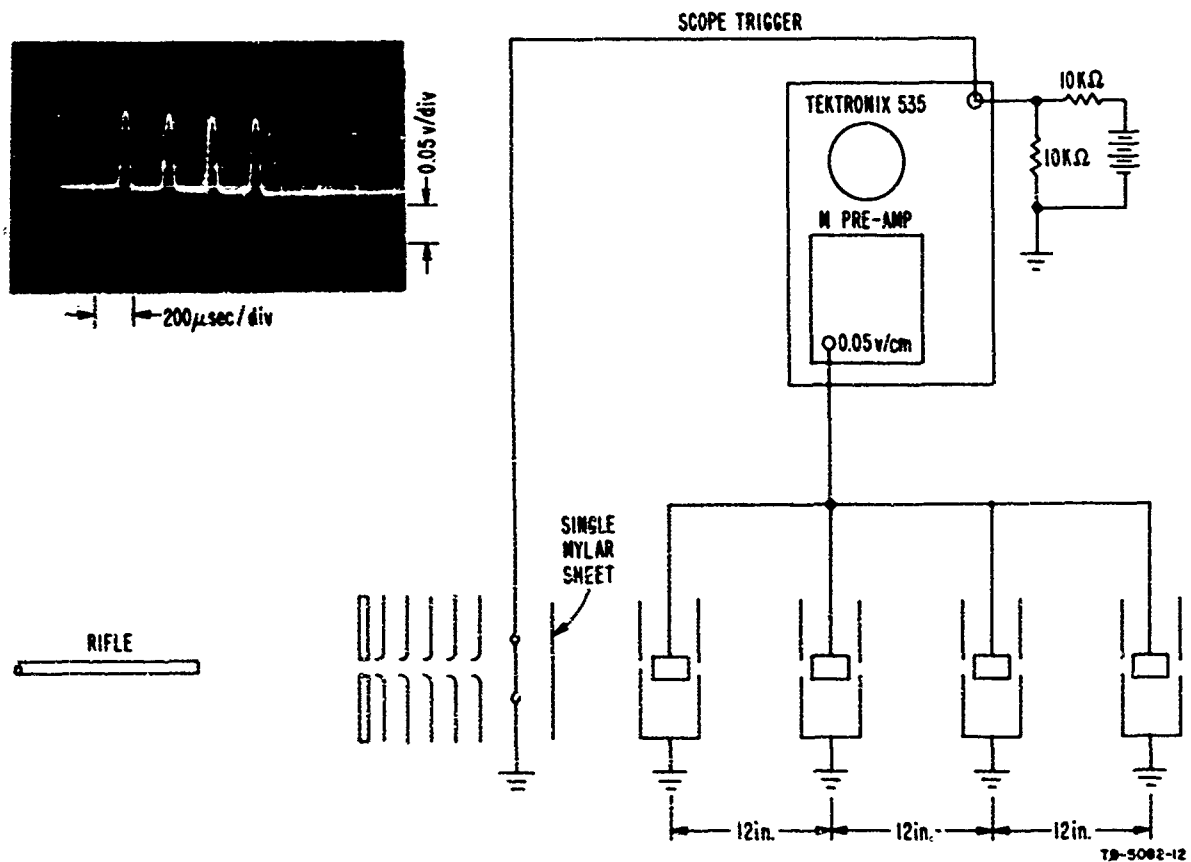


FIG. 13 SET-UP FOR TRACKING PROJECTILE

step-by-step history of projectile progress. The velocity in this case was found to be 4200 feet/sec and did not vary over the instrumented

3-ft-long increment of trajectory. The projectile charge was 113  $\mu\text{coulomb}$  and was constant along the entire trajectory. The gradual depression in pulse peak position on the oscillogram stems from baseline depression which results from the fact that the inequality of Eq. (6) is only partially fulfilled since  $RC = 1.19 \times 10^{-3}$  sec (the oscilloscope input resistance was 1 megohm) and  $l/v = 30 \times 10^{-6}$  sec. With these circuit values, roughly 2.5 percent of the induced charge on the probe flows off during a pulse and serves to depress the baseline by this amount.

#### IV CONCLUSIONS

The primary objective of the research reported here was the development and testing of instrumentation suitable for measuring the electrical charge on a moving projectile. The two probes developed for this purpose were found to be satisfactory. Although the charges measured in these experiments ranged from 50 to 100  $\mu\mu\text{coulomb}$ , greater sensitivity is possible. For example, ten times more sensitivity could have been achieved simply by increasing the oscilloscope gain by a factor of ten.

The parallel plate probe offers a technique for making accurate measurements of projectile velocity, since the output pulse has a well-defined zero crossing from which time measurements can be made. Both probes are attractive for studying moving charged bodies since the probes and their associated instrumentation are quite simple.

## REFERENCES

1. R. L. Tanner and J. E. Nanevicz, "Radio Noise Generated on Aircraft Surfaces," Final Report, SRI Project 1267, Contract AF 33(616)-2761, Stanford Research Institute, Menlo Park, California (September 1956) AD 109651.
2. R. L. Tanner and J. E. Nanevicz, "Precipitation Charging and Corona-Generated Interference in Aircraft," AFCRL 336, Tech. Report 73, SRI Project 2494, Contract AF 19(604)-3458, Stanford Research Institute, Menlo Park, California (April 1961) AD 261029.
3. J. E. Nanevicz, E. F. Vance, R. L. Tanner, and G. R. Hilbars, "Development and Testing of Techniques for Precipitation Static Interference Reduction," ASD-TR-62-38, SRI Project 2848, Final Report on Contract AF 33(616)-6561, Stanford Research Institute, Menlo Park, California (January 1962) AD 272807.
4. R. J. Brun and R. G. Dorsch, "Impingement of Water Droplets on an Ellipsoid with Fineness Ratio 10 in Axisymmetric Flow," NACA Tech. Note 3147, NACA, Washington, D.C. (May 1954).
5. R. G. Dorsch, R. J. Brun, and J. L. Gregg, "Impingement of Water Droplets on an Ellipsoid with Fineness Ratio 5 in Axisymmetric Flow," NACA Tech. Note 3099, NACA, Washington, D.C. (March 1954).
6. R. J. Brun, H. M. Gallegher, and D. C. Vogt, "Impingement of Water Droplets on NACA 65-208 and 65-212 Airfoils at 4° Angle of Attack," NACA Tech. Note 2952, Washington, D.C. (May 1953).
7. R. Gunn, et al., "Army Navy Precipitation Static Project," Proc. IRE, Vol. 27, pp. 301-306 (May 1946).
8. K. R. Spangenburg, Vacuum Tubes, pp. 482-485 (McGraw Hill Book Co., Inc., New York, 1948).
9. W. Shockley, "Currents Induced by a Moving Charge," J. Appl. Phys., Vol. 9, pp. 635-636 (October 1938).
10. Simon Ramo, "Currents Induced by Electron Motion," Proc. IRE, Vol. 27, pp. 584-585 (September 1939).
11. C. K. Jen, "On the Induced Current and Energy Balance in Electronics," Proc. IRE, Vol. 29, pp. 345-349 (June 1941).
12. J. E. Nanevicz, "A Study of Precipitation-Static Noise Generation in Aircraft Canopy Antennas," Tech. Report 62, SRI Project 1197, Contract AF 19(604)-1296, Stanford Research Institute, Menlo Park, California (December 1957).

13. R. L. Tanner and J. E. Nanevich, "An Analysis of Corona-Generated Interference in Aircraft," Proc. IEEE, 52, No. 1, pp. 44-52 (January 1964).

UNCLASSIFIED

Security Classification

| DOCUMENT CONTROL DATA - R&D  |   |  |
|--|---|--|
| <i>(Security classification of title, body of abstract and indexing annotation must be entered when the overall report is classified)</i>  |   |  |
| 1. ORIGINATING ACTIVITY (Corporate author)<br><br>Stanford Research Institute<br>Menlo Park, California  |   | 2a. REPORT SECURITY CLASSIFICATION<br><br>Unclassified |
|  |   | 2b. GROUP  |
| 3. REPORT TITLE<br><br>MEASURING THE ELECTRICAL CHARGE AND VELOCITY OF A MOVING PROJECTILE   |   |  |
| 4. DESCRIPTIVE NOTES (Type of report and inclusive dates)<br><br>Interim Engineering Report 1  |   |  |
| 5. AUTHOR(S) (Last name, first name, initial)<br><br>Nanevicz, Joseph E.      Wadsworth, Willard C.  |   |  |
| 6. REPORT DATE<br><br>January 1965   | 7a. TOTAL NO. OF PAGES  | 7b. NO. OF REFS  |
| 8a. CONTRACT OR GRANT NO.<br><br>AF33(615)1934   | 9a. ORIGINATOR'S REPORT NUMBER(S)<br><br>Interim Engineering Report 1   |  |
| b. PROJECT NO.   | 9b. OTHER REPORT NO(S) (Any other numbers that may be assigned this report)   |  |
| c.   | SRI Project 5082  |  |
| d.   |   |  |
| 10. AVAILABILITY/LIMITATION NOTICES  |   |  |
| 11. SUPPLEMENTARY NOTES  | 12. SPONSORING MILITARY ACTIVITY<br>Air Force Avionics Laboratory<br>Research and Technology Division<br>USAF, Wright-Patterson AFB, Ohio |  |
| 13. ABSTRACT<br><br>Two different probes were developed for measuring the electrical charge and velocity of a moving charged projectile. The probes were tested using 5/32-inch-diameter steel balls fired from a rifle at roughly 4500 feet per second. The projectiles were frictionally charged to from 50 to 100 $\mu$ coulomb by passing through a 0.0003-inch-thick plastic sheet. |   |  |